

RESPONSE OF PASSIVE MICROWAVE SEA ICE CONCENTRATION ALGORITHMS TO THIN ICE

Georg Heygster¹, Marcus Huntemann¹, Natalia Ivanova⁴, Roberto Saldo³, Leif Toudal Pedersen²

¹Institute of Environmental Physics, University of Bremen, ²Danish Meteorological Institute
³Technical University of Denmark, ⁴Nansen Environmental Research Center, Bergen, Norway

ABSTRACT

The influence of sea ice thickness brightness temperatures and ice concentrations retrieved from passive microwave observations is quantified, using horizontally homogeneous sea ice thickness retrievals from ESA's SMOS sensor observations at high incidence angles. Brightness temperatures are influenced by thickness below 18 cm (89GHz) and 50 cm (1.4 GHz). Ice concentration retrievals reduced by ice thickness below 0.17 m and 0.33 m, with higher frequency algorithms being less influenced.

Index Terms — sea ice thickness, SMOS, L-band, sea ice concentration retrieval, passive microwave

1. INTRODUCTION: RELEVANCE OF THIN SEA ICE

The thickness of sea ice influences its thermodynamic (heat transfer between ocean and atmosphere), radiative (albedo) and dynamic (resistance against the deforming forces of wind and waves) properties. The sensitivity of these processes to thickness changes is highest at low thickness. Moreover, the navigating capability of ships in ice depends (according to their ice class) on the ice thickness. The area of Arctic ice new formed in each season has been increasing continuously by about 50% over the last four decades as the yearly sea ice minimum extent decreased much faster than that of the maximum. Recently, two methods to infer the thickness recently formed sea ice up to about 0.5 m have been suggested, both based on observations of ESA's L-band sensor SMOS (Soil Moisture and Ocean Salinity). While the algorithm by [1] uses intensities of low incidence angle (0°-40°), the here used algorithm by [2] employs both intensity and polarization difference between 40° and 50° degree incidence angle. For the sake of simplicity, here we will call all undeformed ice up to 50 cm 'thin ice', comprising the WMO sea ice homogeneous types nilas, young ice (0.1-0.3 m) and partly first-year ice (0.3-1.5 m).

Sea ice concentration, i.e. the percentage of sea ice covered surface, has been observed from space since over

30 years with multichannel passive microwave sensors, and almost as long it is known that the retrieved ice concentration is influenced by the thickness of thin sea ice. While the emissivity of first-year and multiyear has been investigated massively (e.g. [6]), the spillover of the thickness of thin ice to sea ice concentration has never been investigated quantitatively. Here, in the context of sea ice project of ESA's Climate Change Initiative [3], the influence of the sea ice thickness on the observed brightness temperatures is investigated, and from the latter, the influence on the sea ice concentration retrievals from various algorithms is determined. In total, 29 sea ice concentration (SIC) algorithms have been implemented and applied. See [4] for definition and description of the algorithms.

2. THIN SEA ICE DATA SETS

Two data sets of thin sea ice have been compiled, one based on SMOS retrieved sea ice thickness (SIT) alone, and one using SAR data in addition. In order to compare the selected SIC algorithms, several data packages of brightness temperatures observed by AMSR-E under specific conditions have been prepared, such as open water, 100% ice concentration, or with a specific percentage of melt ponds. Here we use a data set where the sea ice thickness as determined from SMOS observations was homogeneous within a standard deviation of 2 cm over a Region of Interest (RoI) of 7x7 pixels, each 12.5x12.5 km, of a polar stereographic grid with equal area at 70° latitude into which the retrieved SMOS thicknesses were projected. Initially, the homogeneity condition was extended in addition over 3 consecutive days. However, it turned out that the maximum thickness fulfilling this constraint was about 0.3 m, so that the time constraint was abandoned. The original SMOS Level 1c (L1c) data, version 5.05, are available in the SMOS Discrete Global Grid (DGG), an Icosahedral Snyder Equal Area projection with aperture 4 and resolution 9 (ISEA 4H9) of 15x15 km² grid cells. The investigation period was from Nov 2-19, 2010, when the extent of retrieved thin ice was highest in that Arctic ice

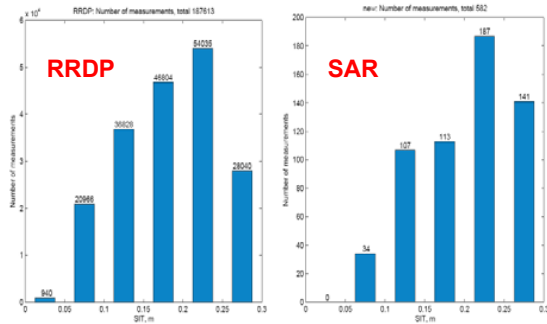


Figure 1: Thickness distributions of the two used thin sea ice data sets.

season. Prior to determining the sea ice thicknesses, the SMOS LIC data were converted from the instrument to the surface reference frame [2] and daily averaged. The thus obtained data set, called Round Robin Data Package (RRDP) comprises 187,613 cells of the polar stereographic grid. The constraint of standard deviation below 2 cm in the RoI ensures the large-scale homogeneity of the retrieval.

In order to also exclude sub-pixel inhomogeneities of the sea ice cover, a subset of this data set was generated, where in addition the homogeneity within the considered pixel was checked by visual inspection of in total 175 ENVISAT ASAR WSM SAR (Wide Swath Mode data of ENVISAT's Advanced SAR) scenes taken on the same day. The thus obtained subset of thin sea ice data, called SAR data set, comprises 582 pixels in total. The thickness distribution of both data sets (Fig. 1) is has a maximum in the range of 0.2 to 0.25 m. The bin 0 to 0.05 m SIT is not occupied in the SAR data set. To each of the two data sets, stored as line wise ASCII files with sea ice thickness, latitude, longitude and date, first the corresponding daily averaged AMSR-E brightness temperatures were added, and then the SIC values as obtained from the 29 retrieval algorithms.

3. RESULTS

3.1. Brightness temperatures

The resulting brightness temperatures of the SAR data set for the AMSR-E frequencies 6, 10, 18, 22, 37 and 89 GHz and both polarizations as function of SIT, binned in 5 cm intervals, are shown in Figure 2 together with the corresponding polarization differences (vertically minus horizontally polarized). In addition, the 1.4 GHz curves as obtained from SMOS are shown. Features common to both data sets (the RRDP data set not shown here) are the decrease of the brightness temperatures and the increase of the polarization difference as the SIT approaches 0 m. Complementing the curves at SIT 0 m with the values of the

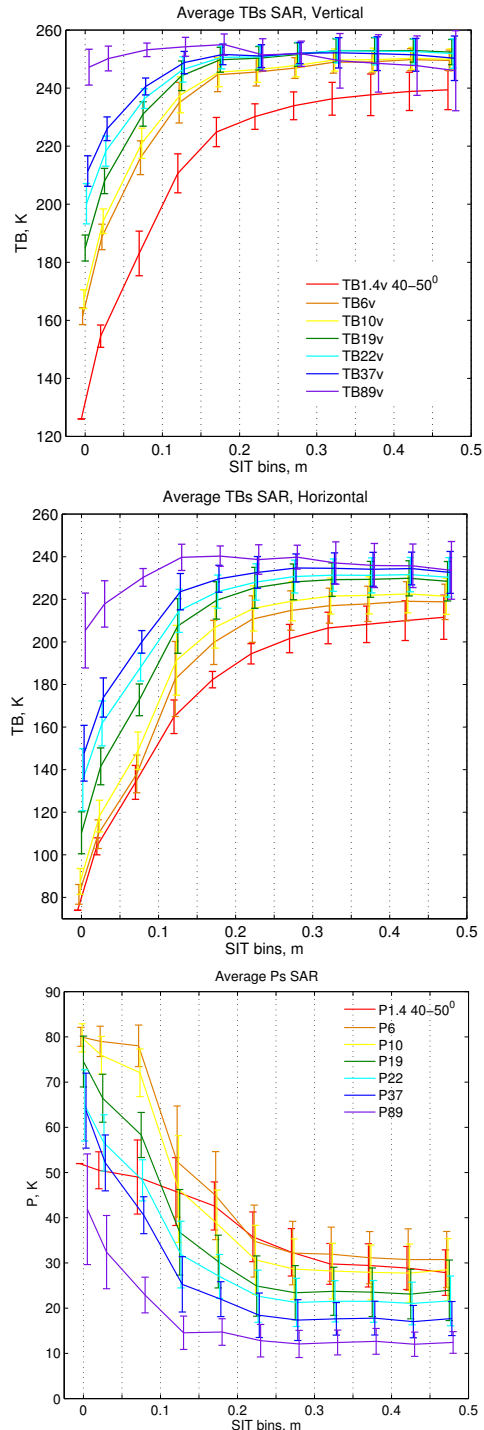


Figure 2: Vertically (top), horizontally (middle) polarized brightness temperatures and polarization difference (bottom) as function of sea ice thickness, various frequencies.

open water RRDP as shown in Figure 2 results in monotonous extensions except at 89 GHz, both polarizations, and the corresponding polarization difference. The decrease of the brightness temperatures (TBs) starts between 0.18 (89V) and 0.33 m (19H) in the RRDP data set (not shown) and in the SAR data set between 0.08 m (89V) and 0.28 m (6H). In both data sets, the lower microwave frequencies are more sensitive to SIT changes than the higher ones, and the transition from the brightness temperatures at 0 m ice thickness (open water) to 0.08m shows the strongest TB change. All TBs increase with sea ice thickness except those at 89 GHz where a small decrease of about 5 K from 0.18m to 0.5m at v-pol and of about 10 K at h-pol. However, the polarization difference keeps decreasing monotonically up to 0.5b m thickness at all investigated frequencies.

We attribute the increase of the standard deviations of the observed TBs increasing with thickness to the increase of the variability of the sea ice cover with thickness and to the reducing sensitivity of the SMOS based thickness retrieval procedure which reaches its limit near 0.5 m thickness. The differences between the two data sets (not shown here) are higher at horizontal than at vertical polarization and they are below 5 K for SIT>0.3 m at both brightness temperatures and polarization difference. At 89 GHz, the difference between the polarization differences of the two data sets reaches -20K at 0.08 m SIT. This inconsistency is currently unexplained and investigated in more detail.

3.2 Sea ice concentration

Figure 3 (top) shows the result of applying the 29 sea ice concentration algorithms to both data sets. The color of the lines indicates SIC retrievals. Ideal algorithms would return 100% SIC for all positive thicknesses and 0 for open water. In the RRDP data set, the influence of the SIT on the SIC is visible at thicknesses below 0.17 and 0.3 depending on the algorithm, while in the SAR data set the SIT influences the SIC only at thicknesses below 0.13 and 0.23 m depending on the algorithm. Figure 3 (bottom) shows the SIC estimates of the algorithms at 0.25 m SIT for the RRDP data set. The ordered sequence of ice concentrations retrieved at 0.25 m SIT in Figure 3 (bottom) shows that the SIC algorithms based on the highest microwave frequency, 89 GHz (Near_90_lin_dyn, Near90GHz, P90, ASI), are generally less influenced by the SIT, and those involving lower microwave frequencies are stronger influenced (P10, One channel (6GHz)). This is in agreement with the low influence of thickness at 89 GHz (Fig. 2). The least sensitivity to sea ice thickness is shown by the ASI algorithm [5] which uses a 3rd order polynomial applied to the near 90 GHz polarization difference. This effect may in part be due to the low slope of the 3rd order polynomial retrieval curve (ice concentration as function of polarization

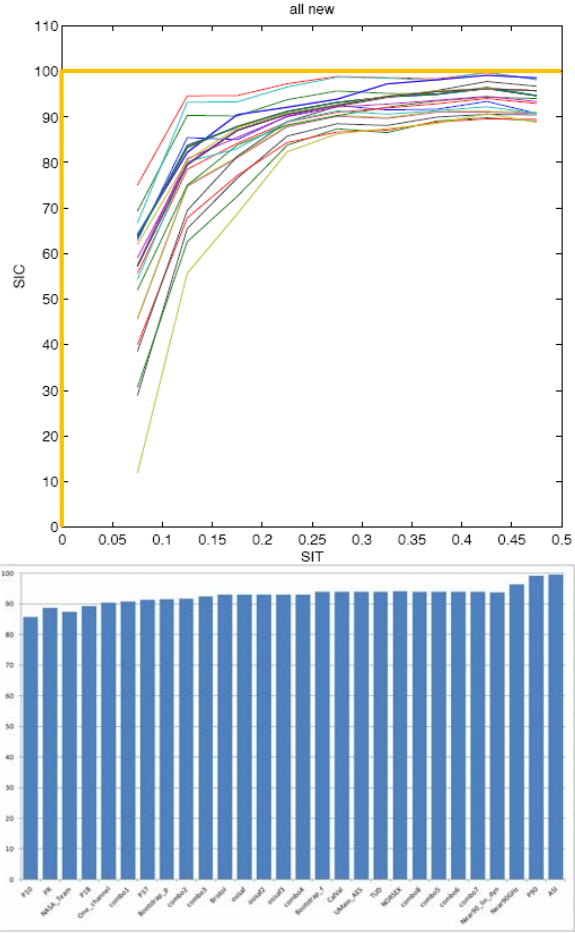


Figure 3: Top: Sea ice concentrations as retrieved from 29 algorithms. The yellow line indicates the behavior of an ideal algorithm. Bottom: SIC estimates of the various algorithms at 0.25 m SIC RRDP data set. The sequence of algorithms is given Table I.

difference) at high ice concentrations. As a result, the algorithm is little sensitive at ice concentrations near 100%.

4. DISCUSSION AND CONCLUSIONS

The brightness temperature as function of SIT decreases in both data sets in a qualitatively similar way towards 0 SIT, but the sensitivity to thickness starts in the RRDP data set at higher thickness values than in the SAR data set. A potential explanation can be parts of open water present in some pixels of the RRDP data set. Such pixels would have been excluded in the SAR data set by the homogeneity check. In line with the behavior of the brightness temperatures, also the retrieved SICs are influenced by the

Table I: Order of sensitivity of sea ice algorithms to thickness of thin ice (Fig. 3 bottom). Most sensitive algorithms at top.

Column 1	Column 2	Column 3
P10	Combo3	NORSEX
PR	Bristol	Combo8
NASA-Team	Osisaf	Combo6
P18	Osisaf3	Near 90 lin dyn
One channel	Combo4	Near90GHz
Combo1	Bootstrap f	P90
P37	calVal	ASI
Bootstrap p	UMass AES	
Combo2	TUD	

SIT, and the influence is stronger for algorithms involving lower frequency channels and lowest for those relying uniquely on the highest microwave frequency, 89 GHz. The answer of sea ice algorithms to thin ice is just one aspect in judging their quality. Other aspects involve the reliability to detect open water, 100% SIC or their sensitivity to melt ponds in Arctic summer sea ice. All these aspects are taken together to select the algorithm used to establish the ESA Climate Change Initiative time series of sea ice concentration.

5. ACKNOWLEDGEMENT

This activity has been made possible by the ESA Sea Ice Climate Change Initiative (SICCI) under contract 400010733/I-AM.

6. REFERENCES

- [1] Kaleschke, L., X. Tian-Kunze, N. Maaß, M. Mäkynen, and M. Drusch (2012), Sea ice thickness retrieval from SMOS brightness temperatures during the Arctic freeze-up period, *Geophys. Res. Lett.*, doi:10.1029/2012GL050916.
- [2] M. Huntemann, G. Heygster, L. Kaleschke, T. Krumpen, M. Mäkynen, and M. Drusch: Empirical sea ice thickness retrieval during the freeze up period from SMOS high incident angle observations. *The Cryosphere*, 8, 439-451, doi:10.5194/tc-8-439-2014.
- [3] SICCI 2012: ESA CCI Sea Ice website esa-cci.nerisc.no.
- [4] Ivanova, N. Algorithm Theoretical Basis Document (version 1): Sea Ice Concentration for SICCI project. Technical report, NERSC, Bergen, 66 pages, 2013.
- [5] G. Spreen, L. Kaleschke and G. Heygster 2008: Sea ice remote sensing using AMSR-E 89 GHz channels. *J. Geophys. Res* 113, C02S03, doi:10.1029/2005JC003384.
- [6] Mathew, N., G. Heygster, and C. Melsheimer 2009: Surface emissivity of the Arctic sea ice at AMSR-E frequencies. *IEEE Trans. Geosci. and Remote Sensing* 47(12), p. 4115-4124, doi:10.1109/TGRS.2009.2023667.